



On the possible formation of Alfvén wings at Mercury during encounters with coronal mass ejections

Menelaos Sarantos¹ and James A. Slavin¹

Received 21 November 2008; revised 9 January 2009; accepted 26 January 2009; published 26 February 2009.

[1] The solar wind conditions near Mercury's perihelion, especially during Interplanetary Coronal Mass Ejection (ICME) events, will often be characterized by very low Alfvén Mach number (≤ 3). We suggest that the low Mach numbers and large north-south magnetic fields during ICMEs will lead to the formation of "Alfvén wings" that will affect the configuration of the Hermean magnetosphere. It is shown that an electrical conductance threshold of about 5 S, comparable to the Alfvén conductance in the solar wind, is required for generation of Alfvén wings at Mercury. Assuming crustal conductances above this value it is demonstrated that currents in the Alfvén wings and closing across the planetary surface will produce significant perturbations (≥ 10 nT) of the magnetospheric magnetic field. **Citation:** Sarantos, M., and J. A. Slavin (2009), On the possible formation of Alfvén wings at Mercury during encounters with coronal mass ejections, *Geophys. Res. Lett.*, 36, L04107, doi:10.1029/2008GL036747.

1. Introduction

[2] Measurements by the MESSENGER spacecraft, obtained during its first Mercury flyby, show a reconnecting magnetosphere immersed in an extended cloud of neutrals and ions of planetary origin [Slavin *et al.*, 2008; Zurbuchen *et al.*, 2008]. A number of analytic, magnetohydrodynamic (MHD), and hybrid models have previously examined the interaction of this magnetosphere with the solar wind (see review by Slavin [2004]). However, the external conditions assumed in these simulations do not generally extend to the low Mach number regime which will be typical of conditions around Mercury's perihelion or during solar outbursts. These expectations, along with recent work detailing the interaction of the Earth's [Ridley, 2007; Kivelson and Ridley, 2008] and Ganymede's [Jia *et al.*, 2008] magnetosphere with low Alfvén Mach number (M_A) plasma flows, have prompted us to investigate the electrodynamic interaction of Mercury's magnetosphere with the solar wind for $M_A < 3$.

[3] An electrically conducting body in a magnetized flowing plasma will become an obstacle to that flow through the induction of shielding currents which exclude the incident magnetic flux tubes and cause them to bend as they slip past the body. Fast-mode, slow-mode and shear Alfvén waves are launched by this interaction, with the latter travelling unattenuated along the bent fieldlines, which act as "transmission" lines. In the MHD approximation the Alfvén waves

dominate the far-field radiation field and the extended sheets of current are called Alfvén wings [Drell *et al.*, 1965].

[4] The perturbation of the magnetic field due to Alfvén wings is proportional to the effective conductance of the obstacle and intensifies at low Alfvén Mach numbers. These structures have been observed at many inner Jovian Moons which lie in sub-Alfvénic flow [see Kivelson, 2004, and references therein]. The conducting obstacle may be an ionosphere (e.g., Io, Europa) or some combination of the ionosphere and/or mildly conducting planetary surface with an internal magnetic field (Ganymede). Neubauer [1998] qualitatively described how the Alfvén wings are modified by Ganymede's reconnecting magnetosphere. These ideas have been further corroborated by the self-consistent MHD modeling of Jia *et al.* [2008]. MHD simulations have also predicted the formation of Alfvén wings in the terrestrial magnetosphere when strongly southward interplanetary magnetic field (IMF) conditions are combined with unusually low Alfvén Mach number (< 3) flows as are common during major interplanetary coronal mass ejections (ICMEs) [Ridley, 2007].

[5] Data from the inner heliosphere, obtained by the Helios spacecraft (1975–1981), indicate that conditions prevailing at Mercury have similarly low Alfvén Mach number [e.g., Russell *et al.*, 1988]. This leads to the possibility, which is explored in this paper, that Alfvén wings may at times mediate the interaction of the solar wind with Mercury's magnetosphere provided that the planet is sufficiently conductive.

2. Observed Plasma Parameters at Mercury

[6] Properties of the solar wind plasma that describe its interaction with Mercury's magnetosphere include: the Alfvén and sonic Mach numbers, which are the ratios of the solar wind speed (V_{SW}) to the Alfvén (V_A) and sonic (V_S) speeds, respectively; the solar wind pressure; the plasma beta, defined as the ratio of thermal plasma pressure to the magnetic field pressure; the Alfvén conductance, $\Sigma_A = (\mu_0 V_A)^{-1}$; and the magnitude of the IMF [Russell *et al.*, 1988; Slavin, 2004]. Due to the high eccentricity of Mercury's orbit, plasma and field parameters vary greatly during a Hermean year [Sarantos *et al.*, 2007]. Here we focus on the derivative parameters around the perihelion range (0.31–0.35 AU), where the Alfvén Mach number is lowest.

[7] The sonic Mach number, M_S , the solar wind pressure, P_{SW} , and Alfvén conductance, Σ_A , are presented in Figure 1 as a function of the Alfvén Mach number, M_A . Since $M_A \propto M_S \sqrt{\beta}$, $M_A \propto \sqrt{P_{SW}/B_{SW}}$, and $M_A \propto V_{SW} \Sigma_A$, contours of constant plasma beta, the IMF magnitude and of the solar wind velocity, respectively, have been overlaid to guide the reader. It is seen that the typical plasma conditions at

¹Heliophysics Science Division, NASA Goddard Space Flight Center, Greenbelt, Maryland, USA.

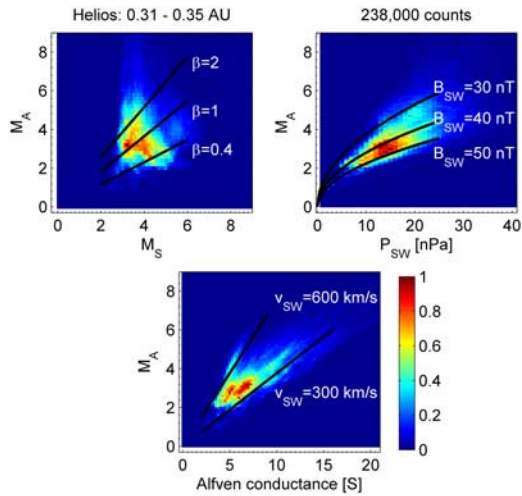


Figure 1. Relative frequency of solar wind properties at heliocentric distances around Mercury’s perihelion (0.31–0.35 AU). At the inner “leg” of the orbit the solar wind–Hermean magnetosphere interaction is expected to be dominated by low Mach number conditions.

Mercury’s perihelion fall into the following regimes: $2 \leq M_A \leq 4$, $3 \leq M_S \leq 6$, $5 \text{ nPa} \leq P_{\text{SW}} \leq 25 \text{ nPa}$, $0.4 \leq \beta \leq 2$, $30 \text{ nT} \leq B_{\text{SW}} \leq 50 \text{ nT}$, and $300 \text{ km/s} \leq V_{\text{SW}} \leq 600 \text{ km/s}$. The solar wind Alfvén conductance, a proxy for the conductance on open field lines of the magnetosphere, is estimated to be $\sim 4\text{--}8 \text{ S}$.

[8] However, the Alfvén Mach number could be even lower (~ 1) during major ICMEs. Figure 2 displays an example of an ICME encountered by the Helios 1 spacecraft near Mercury’s orbit, i.e. at 0.34 AU from the Sun, on 20 June 1981 [Liu *et al.*, 2005]. Solar wind dynamic pressure and the interplanetary electric field potential drop across a transverse length scale comparable to Mercury’s magnetosphere, i.e. $\sim 1 R_M$, would correspond to $\sim 500 \text{ nPa}$ and 200 kV , respectively, during and just after the arrival of the ICME-driven interplanetary (IP) shock around $\sim 3:30 \text{ UT}$. Strong north–south magnetic fields, at times exceeding $\pm 100 \text{ nT}$, were observed over a $\sim 12 \text{ hr}$ interval. Low Alfvén Mach number conditions, which are typical of the leading part of ICMEs, lasted for several hours after the IP shock passed Helios. The flux rope topology of the ICME would result in large angles between the velocity and magnetic field vectors.

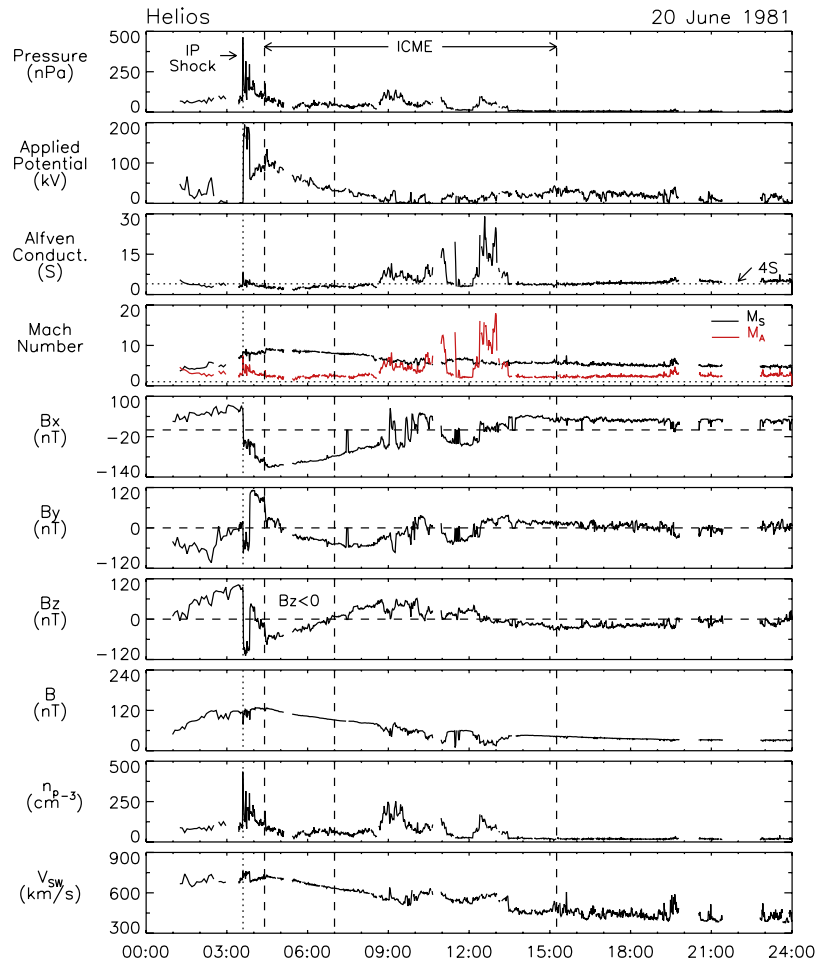


Figure 2. Helios 1 measurements during an ICME observed at 0.34 AU. From top to bottom the panels display: solar wind ram pressure; applied potential drop across a magnetospheric scale length of $1 R_M$, ($-V_{\text{SW}} \times B_{\text{yz}}$). L; solar wind Alfvén conductance; Alfvénic (red) and sonic (black) Mach numbers; the radial (B_x), north-south (B_z) and east-west (B_y) components of the IMF and the total field intensity; and, finally, the solar wind density and speed.

[9] The Alfvén Mach number of ICMEs will generally be lower at Mercury than at 1 AU. The average density inside ICMEs scales as $N(r) \approx r^{-2.32}$, while the magnetic field falls off as $B(r) \approx r^{-1.4}$ and the velocity is nearly constant [Liu *et al.*, 2005]. The resulting Alfvén Mach number of the expanding ICMEs is statistically expected to increase as $M_A(r) \approx r^{0.24}$ out to 1 AU. This result implies that, on average, an ICME having $M_A \sim 3$ at the Earth will have $M_A \sim 2.3$ at Mercury’s perihelion. Sub-Alfvénic solar wind conditions are observed for $\sim 5\%$ of the total time Earth is immersed in ICMEs [Lavraud and Borovsky, 2008], and Mercury should experience flows having $M_A \leq 1$ more frequently.

3. Analytical Model of Alfvén Wing Perturbations at Mercury

[10] The inductive interaction of magnetized plasmas with conducting bodies has been studied both in the MHD approximation and at higher frequencies [see Woodward and McKenzie, 1999, and references therein]. Analytically tractable solutions of the linear MHD disturbance induced by a current source were obtained by Woodward and McKenzie [1999] (hereinafter referred to as WM99) as a function of M_A under the following simplifications: (1) the plasma is incompressible, supporting only shear Alfvén waves; (2) the flow is perpendicular to the uniform background magnetic field; and (3) a point source current, driven through the obstacle, is specified *a priori* pointing to the direction of the motional electric field. Although the flow is generally only 20° – 30° off the ambient field direction at Mercury, assumption (2) is justified at times of ICMEs when large non-radial IMF components are typical (Figure 2).

[11] We use the WM99 model to determine the conditions under which the Alfvén wing magnetic field perturbation becomes comparable to the lobe and magnetosheath magnetic fields. These analytic modelling results are meant to anticipate future numerical simulations and allow us to estimate the dependence of the solar wind interaction with Mercury on M_A . In this model solar wind field lines interact directly with the conductive layers such as the surface and planetary interior, which is analogous to the motion of reconnected (“open”) field lines when the IMF is southward.

[12] If x and y are the directions of the background magnetic field, B_0 , and of the current driven through the conductor, J_0 , respectively, the perturbation magnetic field is (WM99, equation (23)):

$$[B_x, B_y] = -\frac{\mu_0 J_0}{8\pi M_A k} \frac{\partial}{\partial x} \left[\frac{\partial}{\partial x}, \frac{\partial}{\partial y} \right] \left(\log \left\{ \left(r - \frac{M_A z}{k} \right)^2 - x^2/k^2 \right\} \right),$$

where M_A the Alfvén Mach number, $k = \sqrt{1 + M_A^2}$, $[x \ y \ z]$ the Cartesian coordinates, and

$$r = \sqrt{x^2 + y^2 + z^2}.$$

The far-field perturbation in the direction of the flow, V_{SW} , is (WM99, equations (24)–(26) of that paper, excluding the dipole term):

$$B_z = -\frac{\mu_0 J_0}{M_A^2} (I_{Bz1} + I_{Bz2}),$$

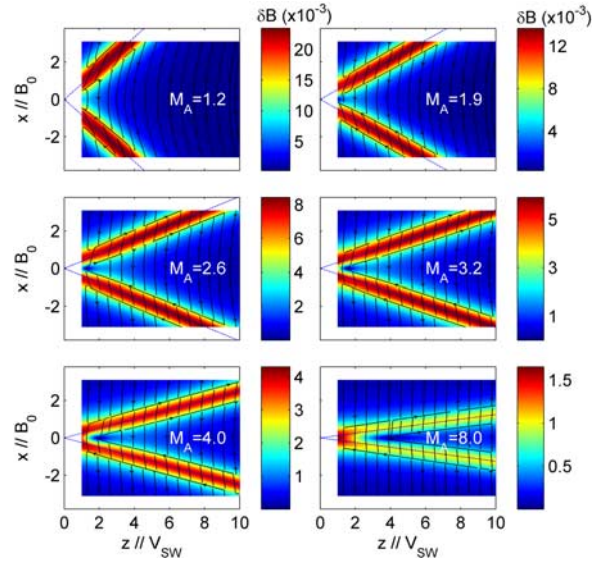


Figure 3. The Alfvénic perturbation of an incompressible plasma in the presence of a current source, assumed to lie at $(0, 0)$ and pointing into the page. The color-coded perturbation magnetic field, in units of $\Sigma_M B_0$, and fieldlines are shown in the $y = 0.5$ plane as a function of the Alfvén Mach number of the plasma flow. The far-field perturbation increases by more than an order of magnitude in going from $M_A = 8$, typical of flows at the Earth, to $M_A \leq 2$ which is expected at Mercury during ICMEs.

where $I_{Bz1} = \frac{M_A^2}{4} \delta(y) [\delta(\zeta_+) + \delta(\zeta_-)]$, and

$$I_{Bz2} = -\frac{1}{8\pi M_A \gamma^2} \left\{ 2\pi \delta(y) [\delta(\zeta_+) - \delta(\zeta_-)] - \frac{1}{2\gamma} \frac{\partial^2}{\partial y^2} \cdot [\log(y^2 + \zeta_+^2/\gamma^2) - \log(y^2 + \zeta_-^2/\gamma^2)] \right\}$$

in which $\zeta_{\pm} = x \pm z/M_A$, and $\gamma = \sqrt{1 + M_A^{-2}}$.

[13] Figure 3 presents the perturbation field magnitude in the $y = 0.5$ plane following these equations. The perturbation clearly increases at low Mach numbers and extends beyond the Alfvén characteristics, whose projection on this plane is shown by blue dotted lines. The current line density, J_0 , can be obtained as $J_0 = \Sigma_M V_{SW} B_0$, where Σ_M is Mercury’s effective conductance. Assuming $V_{SW} = 400$ km/s the maximum perturbation field is $\sim 2 \times 10^{-2} \frac{\Sigma_M}{[13]} B_0$ [nT] for $M_A = 1.2$ and about $\sim 10^{-2} \frac{\Sigma_M}{[13]} B_0$ [nT] for $M_A = 2$. On assuming $\Sigma_M = 5$ S and $B_0 = 100$ nT during an ICME, the field perturbation amounts to ~ 10 and ~ 5 nT, respectively. These perturbations are even higher in the plane containing the Alfvén characteristics ($y = 0$), since in Figure 3 ($y = 0.5$ plane) we have dismissed terms represented by delta functions to avoid singularities. In conclusion, measurable disturbances of the Hermean magnetosphere due to Alfvén waves are in principle possible if the height-integrated conductivity is $\Sigma_M \geq 5$ S. The likely mechanisms for generating electrical conductance of this sort are discussed next.

4. Discussion

[14] The conductivity of Mercury is presently unknown. Due to the highly collisionless nature of Mercury’s exosphere,

Lammer and Bauer [1997] proposed an ionospheric Pedersen conductance of $\sim 5 \times 10^{-6}$ S. Cheng *et al* [1987] estimated a height-integrated pickup ion conductance $\Sigma_P = 0.1\text{--}0.3$ S assuming photoionized sodium to be the dominant ion species. The new measurements by MESSENGER indicate that the sum of relative abundance of ions heavier than 23 atomic mass units (likely Mg^+ , Ca^+ , K^+ and others) is approximately equal to that of Na^+ [Zurbuchen *et al.*, 2008]. The twofold increase of the heavy ion density implies upper limits to the pickup conductance of $\leq 0.3\text{--}0.6$ S.

[15] Although the iron-rich core should be highly conductive, estimates of the regolith and crust conductance vary widely. Conductivities in the range of $10^{-8}\text{--}10^{-4}$ S m^{-1} are often quoted [e.g., Janhunen and Kallio, 2004]. The field lines interact with the surface and with sub-surface layers up to a skin depth. For changes in the solar wind occurring at the typical “frequency” of 10 s (e.g., IMF discontinuities), the corresponding e-folding depth of currents is 159 km; for a magnetic cloud with a southward IMF rotating over 2 hrs, the resulting current layer might be comparable to the mantle thickness. A baseline conductivity of 10^{-4} S m^{-1} , appropriate for lunar crustal materials, was assumed in these calculations yielding an effective conductance of $\Sigma_M = 16$ S for a planar current sheet of 159 km [Janhunen and Kallio, 2004]. Lower and upper limits to the dayside surface conductance of $10^{-2}\text{--}10^2$ S have been estimated over Mercury’s polar caps [Grard *et al.*, 1999]. Surface closure of magnetospheric field-aligned currents was demonstrated by Janhunen and Kallio [2004] assuming $\Sigma_M \leq 16$ S.

[16] The upper limits of Hermean surface conductance estimates can generate Alfvén wings. We may verify this by comparing Mercury to other reconnecting magnetospheres (Ganymede and Earth) during low Alfvén Mach number flows. Strong evidence for the existence of Alfvén wings at Ganymede was provided during several passes by the Galileo probe (see review by Kivelson [2004]). The observed bending-back of the magnetic field in the direction of the corotating plasma flow, as well as the deceleration of the plasma flow from ~ 0.8 (upstream) to ~ 0.3 (polar caps) of the ambient plasma speed, are consistent with the Alfvén wing model. Modeling of the Galileo measurements using a global MHD simulation shows the development of Alfvén wings assuming the effective ionosphere conductance of $\Sigma_G \sim 2$ S [Jia *et al.*, 2008]. The formation of Alfvén wings was also demonstrated in MHD simulations of the Earth’s magnetosphere under strong interplanetary magnetic fields [Ridley, 2007]. In this case the conducting obstacle is the terrestrial ionosphere, whose typical Pedersen conductance is 10 S.

[17] Reconnected field lines of the Earth and Mercury are attached to the solar wind and to the terrestrial ionosphere or the Hermean surface, respectively. Over the polar caps the lower foot of each line is retarded by the conductive medium while the other foot moves at the reconnection velocity. Waves are launched as a result of magnetic tension. Because the upper end of the Hermean field line moves faster than the corresponding end of the terrestrial line as a result of the higher reconnection efficiency at Mercury [e.g., Slavin, 2004], its deformation will be greater assuming the near-surface Hermean conductance to be comparable to the terrestrial Pedersen conductance of 10 S. At Ganymede comparable field line distortions can result from a lesser line-tying con-

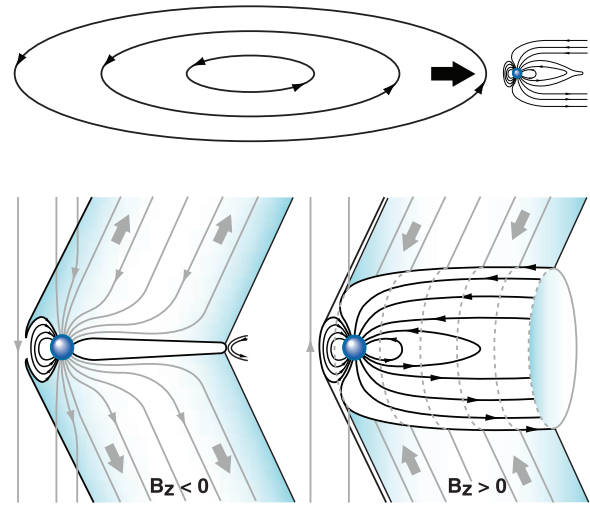


Figure 4. Schematic of the proposed interaction of a CME with Mercury (upper panel) under (left) southward and (right) northward IMF conditions.

ductance since at the “open” end the line is immersed in the sub-Alfvénic Jovian plasma with $M_A \sim 0.5$, moving faster than the Hermean line due to even more efficient reconnection. Evidently, Mercury is an intermediate case between Ganymede and the Earth. Therefore, the minimum Mercury conductance required to sustain Alfvén wings can be constrained as $2 \text{ S} < \Sigma_M < 10 \text{ S}$, i.e. consistent with values obtained in Section 3.

[18] Figure 4 presents a schematic of the resulting Mercury-solar wind interaction during ICMEs. When the prevailing IMF is southward, Alfvén wings form and the interaction looks much like Ganymede [e.g., Neubauer, 1998] and possibly the Earth under similar conditions [Ridley, 2007], where the $j \times B$ force inside the wings decelerates the plasma, while magnetic tension behind the wings re-accelerates it. For northward IMF the currents are excluded from entering the magnetosphere, which is presented as a “bubble”, and they close instead through the magnetopause. The effective conductance which is necessary for this type of interaction must be comparable to the Alfvén conductance.

[19] Kivelson and Ridley [2008] suggested that as the Earth’s ionospheric conductance surpasses the solar wind Alfvén conductance with decreasing Mach number, the applied potential to the magnetosphere is limited by means of partial reflection of Alfvén waves by the ionosphere. They estimated the ratio of cross polar cap potential to the applied solar wind potential to be constrained as $\Phi_{PC}/\Phi_{SW} \leq 2\Sigma_A/(\Sigma_P + \Sigma_A)$. For Mercury their approach would indicate that if $M_A < 2$ and $\Sigma_M \sim \Sigma_A$, the Hermean polar cap potential will begin to saturate.

[20] This is different from the Hill *et al.* [1976] model. They argued that when the ionospheric conductance is high, ionospheric Region 1 currents would introduce some additional magnetic field on the dayside magnetopause which, in turn, would reduce the reconnection efficiency. The resulting polar cap potential drop is limited to $\Phi_{PC} \leq \Phi_{SW}/(1 + \Sigma_P/\Sigma_0)$ where the relevant “line-tying” threshold is $\Sigma_0 \sim 20$ S. In their picture rapid convection at Mercury would be limited only if the near-surface conductance were to approach $\Sigma_M \sim 20$ S. We have shown that during ICMEs Alfvén wings

might dominate the solar wind-magnetosphere interaction at Mercury well before this limit is reached.

5. Conclusions

[21] Mercury's magnetosphere can experience extreme conditions during Coronal Mass Ejections with flows reaching $M_A \sim 1$. We hypothesize that Alfvén wings form under these conditions, and our analysis indicates that this would require a height-integrated conductance of ≥ 5 S. The source of field-aligned current may arise either from ion pickup conductance and/or the conductivity of the regolith, crust and upper mantle. However, a conducting surface is the least constrained term and could most likely provide the necessary conductance. The Mercury-solar wind interaction will be modified during ICMEs as the solar wind flow about Mercury is decelerated by the formation of Alfvén wings (Figure 4). The reduction in the cross-magnetosphere electric field due to the Alfvén wings would also reduce the energy transferred into the magnetosphere. While our conceptual picture of Mercury under southward IMF and low Mach number conditions resembles the interaction of Ganymede with Jupiter's magnetosphere, the opportunity to study Alfvén wing formation in a planetary magnetosphere under the combination of northward IMF and low M_A conditions is unique to Mercury. Modeling studies detailing the role of surface conductivity in closing currents at Mercury [e.g., *Janhunen and Kallio, 2004*] should be extended to the previously unexplored low Mach number regime.

[22] **Acknowledgments.** M.S. was supported by the NASA Postdoctoral Program (NPP) Fellowship.

References

- Cheng, A. F., R. E. Johnson, S. M. Krimigis, and L. J. Lanzerotti (1987), Magnetosphere, exosphere, and surface of Mercury, *Icarus*, *71*, 430–440.
- Drell, S. D., H. M. Foley, and M. A. Ruderman (1965), Drag and propulsion of large satellites in the ionosphere: An Alfvén propulsion engine in space, *Phys. Rev. Lett.*, *14*, 171–175.
- Grard, R., H. Laakso, and T. I. Pulkkinen (1999), The role of photoemission in the coupling of the Mercury surface and magnetosphere, *Planet. Space Sci.*, *47*, 1459–1463.
- Hill, T. W., A. J. Dessler, and R. A. Wolf (1976), Mercury and Mars: The role of ionospheric conductivity in the acceleration of magnetospheric particles, *Geophys. Res. Lett.*, *3*, 429–432.
- Janhunen, P., and E. Kallio (2004), Surface conductivity of Mercury provides current closure and may affect magnetospheric symmetry, *Ann. Geophys.*, *22*, 1829–1837.
- Jia, X., R. J. Walker, M. G. Kivelson, K. K. Khurana, and J. A. Linker (2008), Three-dimensional MHD simulations of Ganymede's magnetosphere, *J. Geophys. Res.*, *113*, A06212, doi:10.1029/2007JA012748.
- Kivelson, M. G. (2004), Moon-magnetosphere interactions: A tutorial, *Adv. Space Res.*, *33*, 2061–2077.
- Kivelson, M. G., and A. J. Ridley (2008), Saturation of the polar cap potential: Inference from Alfvén wing arguments, *J. Geophys. Res.*, *113*, A05214, doi:10.1029/2007JA012302.
- Lammer, H., and S. J. Bauer (1997), Mercury's exosphere: Origin of surface sputtering and implications, *Planet. Space Sci.*, *45*, 73–79.
- Lavraud, B., and J. E. Borovsky (2008), Altered solar wind-magnetosphere interaction at low Mach numbers: Coronal mass ejections, *J. Geophys. Res.*, *113*, A00B08, doi:10.1029/2008JA013192.
- Liu, Y., J. D. Richardson, and J. W. Belcher (2005), A statistical study of the properties of interplanetary coronal mass ejections from 0.3 to 5.4 AU, *Planet. Space Sci.*, *53*, 3–17.
- Neubauer, F. M. (1998), The sub-Alfvénic interaction of the Galilean satellites with the Jovian magnetosphere, *J. Geophys. Res.*, *103*, 19,843–19,866.
- Ridley, A. J. (2007), Alfvén wings at Earth's magnetosphere under strong interplanetary magnetic fields, *Ann. Geophys.*, *25*, 533–542.
- Russell, C. T., D. N. Baker, and J. A. Slavin (1988), The magnetosphere of Mercury, in *Mercury*, edited by F. Vilas, C. R. Chapman, and M. S. Matthews, pp. 514–561, Univ. of Ariz. Press, Tucson, Ariz.
- Sarantos, M., R. M. Killen, and D. Kim (2007), Predicting the long-term solar wind ion-sputtering source at Mercury, *Planet. Space Sci.*, *55*, 1584–1595.
- Slavin, J. A. (2004), Mercury's magnetosphere, *Adv. Space Res.*, *33*, 1859–1874.
- Slavin, J. A., et al. (2008), Mercury's magnetosphere After MESSENGER's first flyby, *Science*, *321*, 85–89.
- Woodward, T. I., and J. F. McKenzie (1999), Stationary incompressible MHD perturbations generated by a current source in a moving plasma, *Planet. Space Sci.*, *47*, 545–555.
- Zurbuchen, T. H., M. Raines, G. Gloeckler, S. M. Krimigis, J. A. Slavin, P. L. Koehn, R. M. Killen, A. L. Sprague, R. L. McNutt Jr., and S. C. Solomon (2008), Observations of Mercury's ionized exosphere and plasma environment, *Science*, *321*, 90–92.

M. Sarantos and J. A. Slavin, Heliophysics Science Division, NASA Goddard Space Flight Center, Greenbelt, MD 20771, USA. (menelaos.sarantos-1@nasa.gov)